Supporting Information for

Contrasting solubility and speciation of metal ions in total suspended particulate matter and fog from the coast of Namibia

Chiara Giorio[1,2]*, Anne Monod[3], Valerio Di Marco[2], Pierre Herckes[4], Denise Napolitano[4], Amy Sullivan[5], Gautier Landrot[6], Daniel Warnes[1], Marika Nasti[1], Sara D'Aronco[1], Agathe Gérardin[3], Nicolas Brun[3], Karine Desboeufs[7], Sylvain Triquet[7], Servanne Chevaillier[8], Claudia Di Biagio[7], Francesco Battaglia[7], Frédéric Burnet[9], Stuart J. Piketh[10], Andreas Namwoonde[11], Jean-François Doussin[8], and Paola Formenti[7]

[1] Yusuf Hamied Department of Chemistry, University of Cambridge, Lensfield Road, Cambridge, CB2 1EW, United Kingdom
[2] Dipartimento di Scienze Chimiche, Università degli Studi di Padova, via Marzolo 1, 35131 Padova, Italy
[3] Aix Marseille Univ, CNRS, LCE, Marseille, France
[4] School of Molecular Sciences, Arizona State University, Tempe, Arizona 85287, USA
[5] Department of Atmospheric Science, Colorado State University, Fort Collins, CO 80523, USA
[6] Synchrotron SOLEIL, L'Orme des Merisiers, Saint-Aubin, France
[7] Université Paris Cité and Université Paris Est Creteil, CNRS, LISA, F−75013 Paris, France
[8] Université Paris Est Creteil and Université Paris Cité, CNRS, LISA, F−94010 Créteil, France
[9] CNRM, Université de Toulouse, Météo-France, CNRS, Toulouse, France
[10] Unit for Environmental Science and Management, North-West University, Potchefstroom, North-West, South Africa
[11] Sam Nujoma Marine and Coastal Resources Research Centre, University of Namibia, Henties Bay, Namibia

*Correspondence to: chiara.giorio@atm.ch.cam.ac.uk

S1. Comparison of metal speciation obtained by Visual MinteQ and PITMAP for three fog samples.

Figures S1-S3 show the comparison between the speciation obtained with Visual MinteQ 3.1 and PITMAP for three fog samples for Al(III), Fe(III), Mn(II), Zn(II), Cu(II) and Ni(II). The results of the two models are qualitatively identical except for a couple of species that were not considered in the PITMAP calculations (e.g., ammonia complexes). In quantitative terms, the results show that the concentration of free metal ions calculated by the two models is very similar. The same results have been obtained also for the main complexes, with minor differences in accounting for the protonation of the complex and formation of mixed organic-hydroxide complexes. Minor differences have been observed for species at very low concentrations (< 10^{-8} M) that are not further discussed in this study.

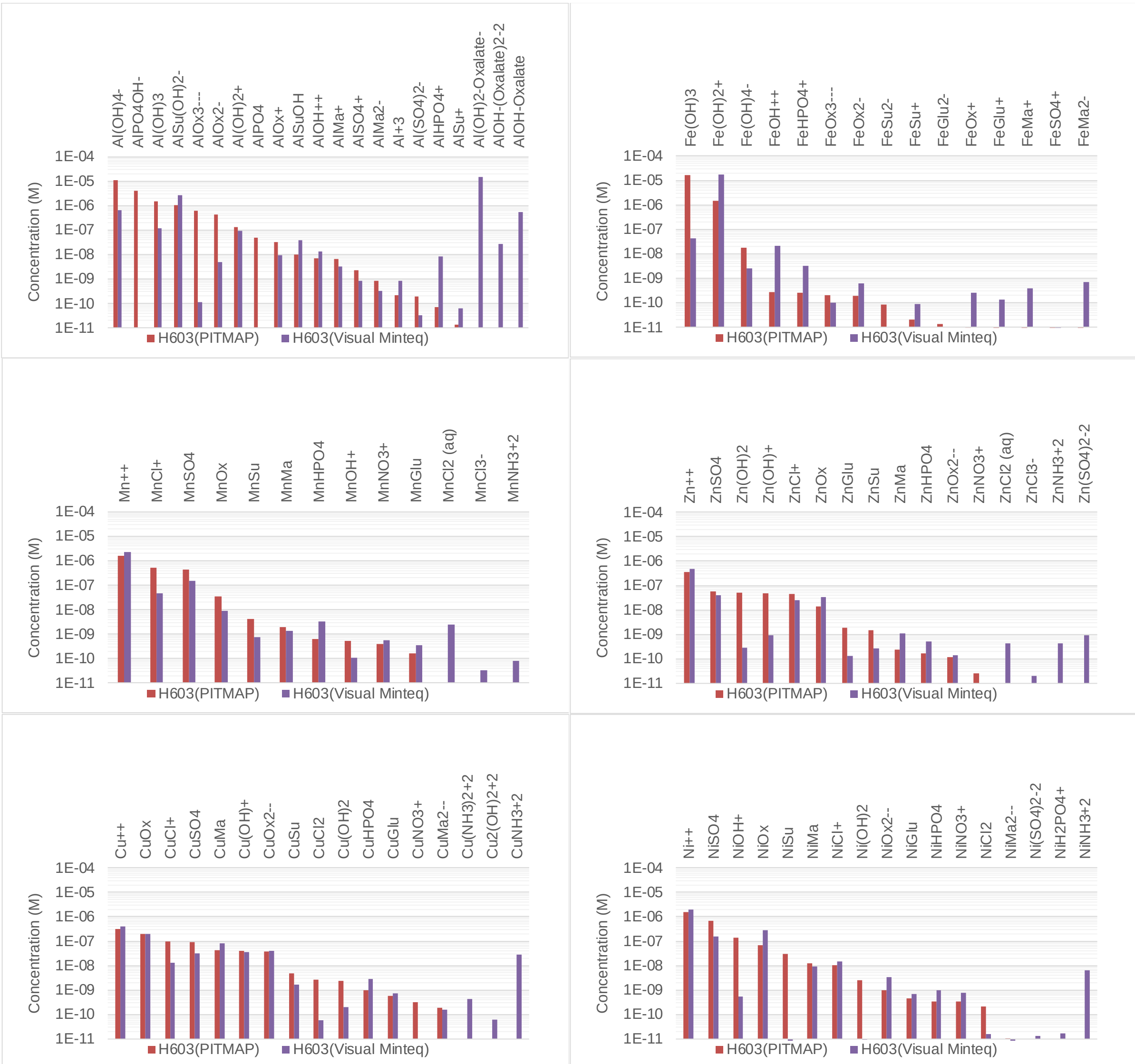

Figure S1. Comparison between the speciation obtained with Visual MinteQ 3.1 and PITMAP for Al(III), Fe(III), Mn(II), Zn(II), Cu(II) and Ni(II) in the fog sample H603.

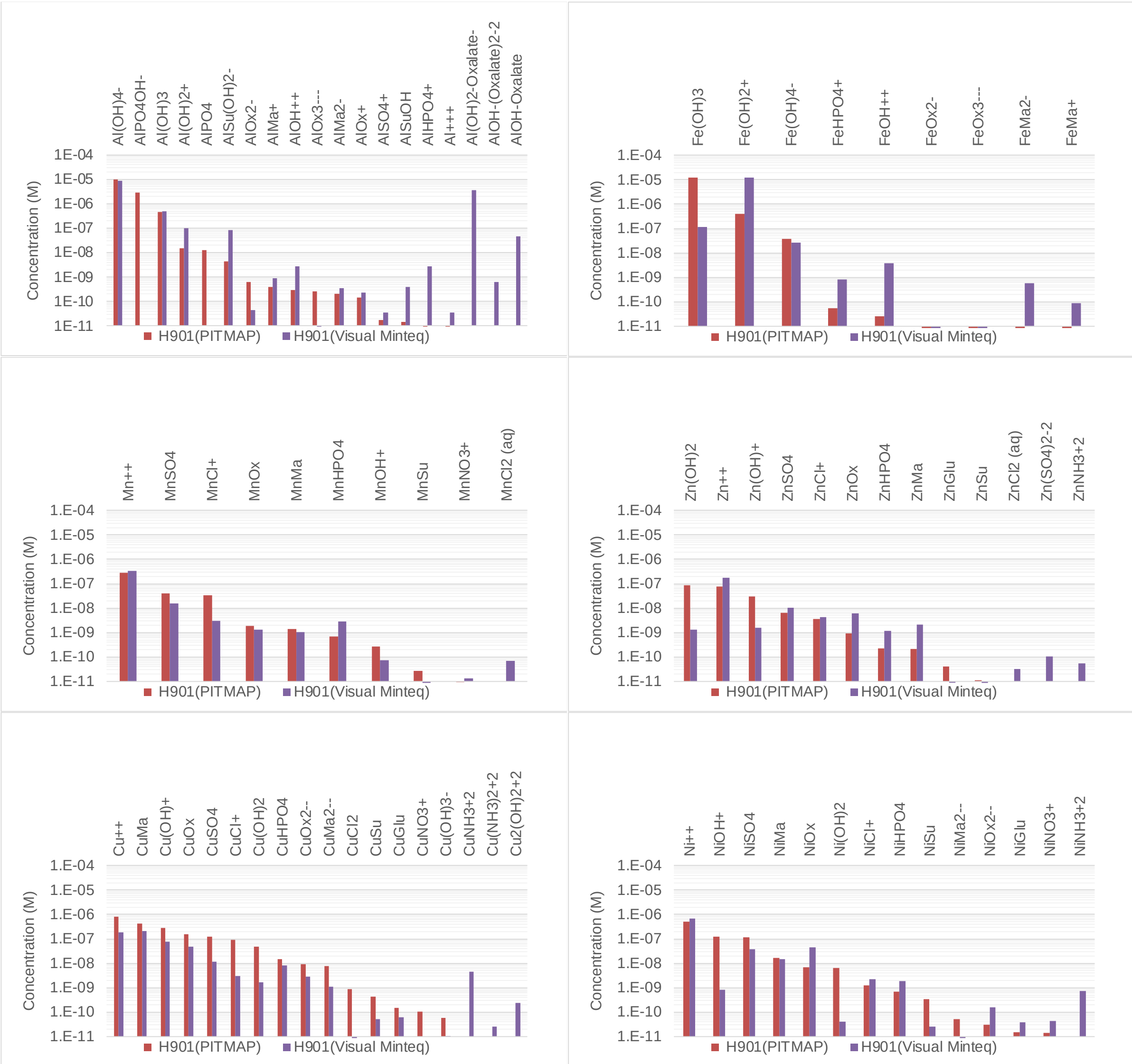

Figure S2. Comparison between the speciation obtained with Visual MinteQ 3.1 and PITMAP for Al(III), Fe(III), Mn(II), Zn(II), Cu(II) and Ni(II) in the fog sample H901.

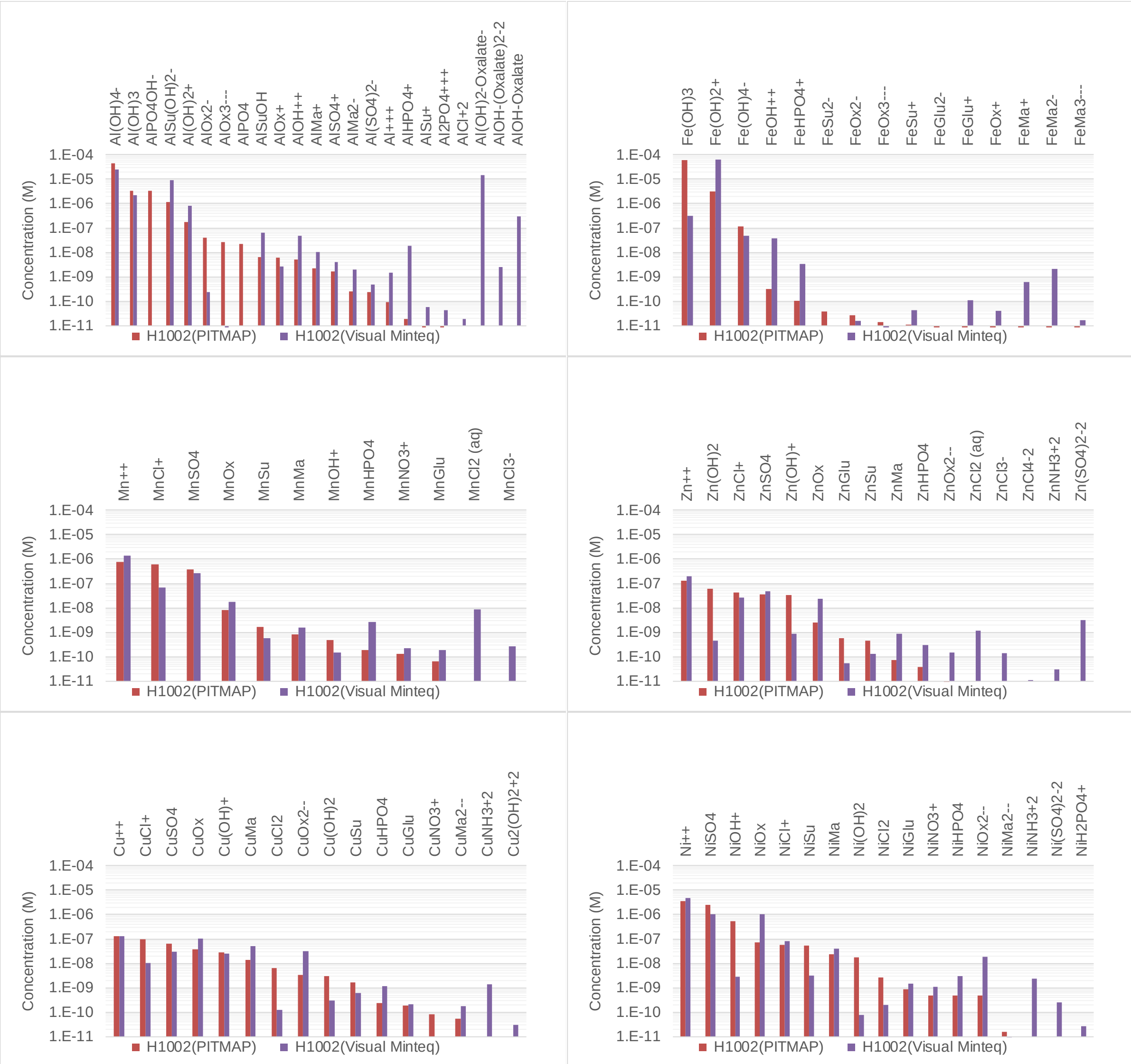

Figure S3. Comparison between the speciation obtained with Visual MinteQ 3.1 and PITMAP for Al(III), Fe(III), Mn(II), Zn(II), Cu(II) and Ni(II) in the fog sample H1002.

S2. Quality-check assessments for fog analysis

A quality-check assessment of the analysis is performed by comparing the concentrations of Mg, K, Ca, Na and Mg^{2+}, K^{+}, Ca^{2+}, and Na^{+} measured by ICP-MS and IC, respectively in all the samples. The comparison reveals an excellent linear correlation between the two datasets, with the coefficient of determination (r^2) exceeding 0.99 for all the elements, with slopes of the linear correlations very close to 1:1. Although phosphate shows high detection limits in IC (55 µg/L), it is measured above this threshold in 11 samples and the comparison with P can be examined. Compared to the above-mentioned elements and ions, P vs PO_4^{3-} (in µM) shows a lower regression fit (r^2=0.79) with a slope of 1.21, showing that a substantial fraction of P is not phosphate. Another quality-check assessment is performed on the major ions to check for the ionic neutrality of all the samples. The comparison shows a linear fit with $r^2 > 0.99$, and a slope of 1.1, slightly higher than 1, probably due to the influence of organic anions. The blanks performed by nebulizing ultrapure water on fog collectors at Henties Bay exhibit median mass concentrations that are always lower than those of fogs for all chemicals: below 2.6 % for the major ions, below 9.1% for trace elements and heavy metals (except for Cr, Co, Ni and Zn, for which the ratio is <40%) and below 11% for organic acids.

S3. Additional results on the fog chemical composition

Table S1. Additional elements measured in fogs and seawater at the coastal site at Henties Bay (complement to Table 2 in the main text).

	Coastal fogs this study				**Coastal seawater this study**
	median	average	min	max	average
Se (µM)	0.045	0.041	0.018	0.060	<LOQ
Rb (µM)	0.17	0.18	0.03	0.32	1.18
Ga (nM)	5.36	4.97	0.98	8.94	0.38
Sb (nM)	1.36	1.62	0.40	3.27	1.28
Cs (nM)	0.70	0.73	0.15	1.16	2.06
La (nM)	12.41	12.73	2.36	22.95	0.80
Ce (nM)	26.77	27.68	4.80	50.31	1.85
Pr (nM)	2.91	2.95	0.54	5.40	0.18
Nd (nM)	11.51	11.59	2.11	21.29	0.69
Sm (nM)	2.30	2.31	0.39	4.23	0.16
Eu (nM)	0.41	0.42	0.07	0.77	0.03
Gd (nM)	1.96	1.95	0.35	3.61	0.14
Tb (nM)	0.27	0.29	0.05	0.55	0.03
Dy (nM)	1.58	1.63	0.27	3.00	0.15
Ho (nM)	0.28	0.29	0.05	0.53	0.02
Er (nM)	0.72	0.77	0.13	1.43	0.08
Tm (nM)	0.10	0.10	0.02	0.18	0.01
Yb (nM)	0.56	0.61	0.11	1.11	0.06
Lu (nM)	0.08	0.08	0.01	0.15	0.01
Hf (nM)	0.06	2.74	0.00	10.83	<LOQ
Re (nM)	0.03	1.36	0.01	8.02	0.07
Tl (nM)	0.20	0.17	0.05	0.25	0.16
Th (nM)	0.56	0.61	0.11	1.12	0.13

The marine source is examined further, using sodium as a tracer and seawater samples as the reference (Figure S4). For each compound X, enrichment factors were calculated using the volume weighed concentrations : $EF_{marine} = \frac{\left({[X]}/{[Na]}\right)_{fog}}{\left({[X]}/{[Na]}\right)_{sea\,water}}$.

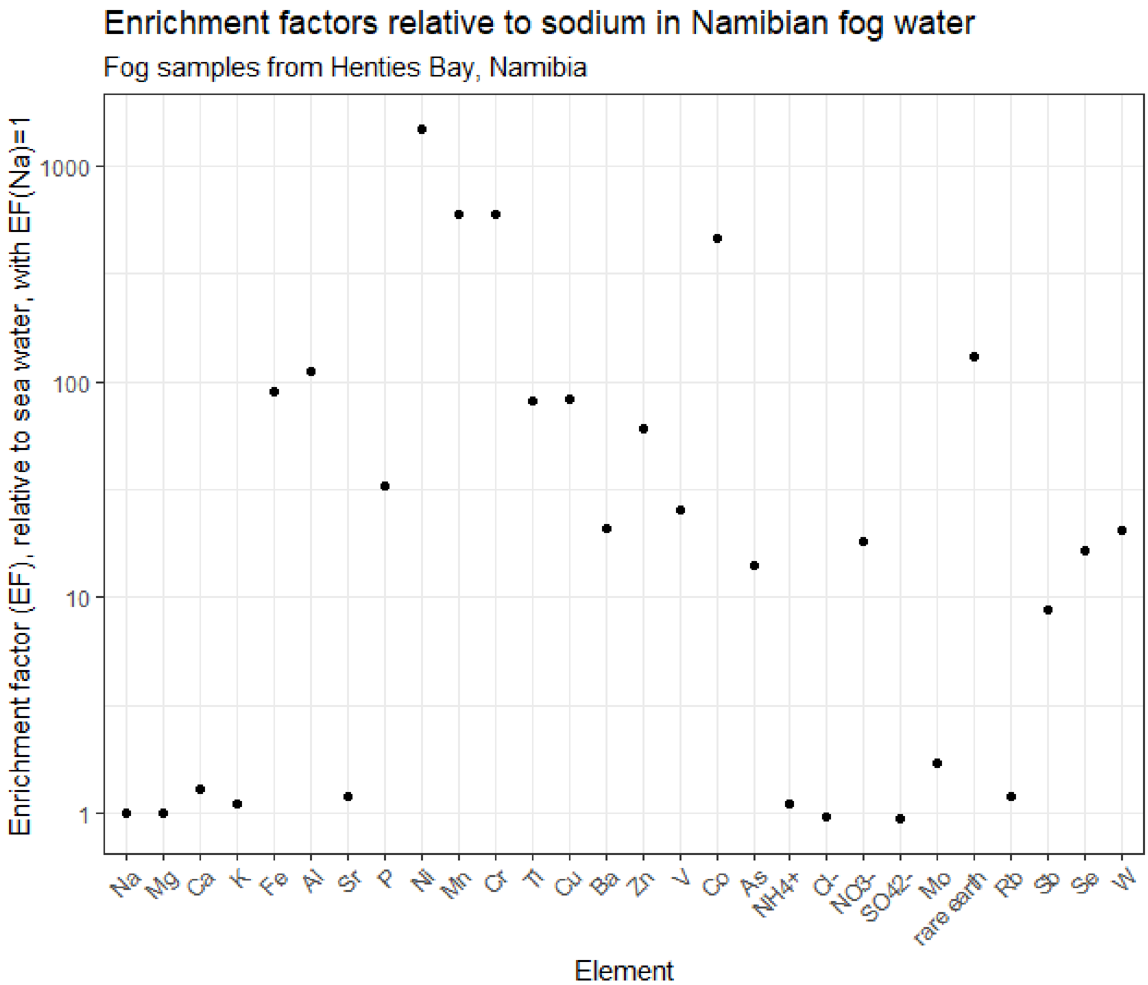

Figure S4. Marine influence on fog chemical composition: enrichment factors for major ions and elements calculated relative to sea water Na on the Volume Weighted Concentrations for all fog samples collected at Henties Bay.

Figure S4 confirms the importance of the marine source, it shows that Cl^-, Mg^{2+}, K^+, SO_4^{2-}, and NH_4^+ are predominantly of marine origin. Figure S4 also shows that Ca, Sr, Rb, and Mo are also highly influenced by marine sources. In addition, MSA shows a moderate correlation with Na^+ (r^2=0.55), comparable to that of sulphate with Na^+ (r^2=0.97), probably due to its secondary atmospheric origin. Figure S4 clearly shows that a number of ions and elements are not exclusively of marine origin. Crustal sources are examined in greater detail. To do so, ions and elements measured in total suspended particles (TSP) are considered. Due to the large influence of marine sources in both fog and TSP samples, non-sea-salt (nss) contributions are calculated, and enrichment factors are calculated relative to nss-Al using as a reference the average nss-ions and nss-elements concentrations measured in TSP (Formenti et al., this issue) over the entire campaign (**Figure S5**). For each compound X, enrichment factors were calculated using the volume weighed concentrations: $EF_{crustal} = \frac{\left({[X]}/{[Al]}\right)_{fog}}{\left({[X]}/{[Al]}\right)_{TSP}}$.

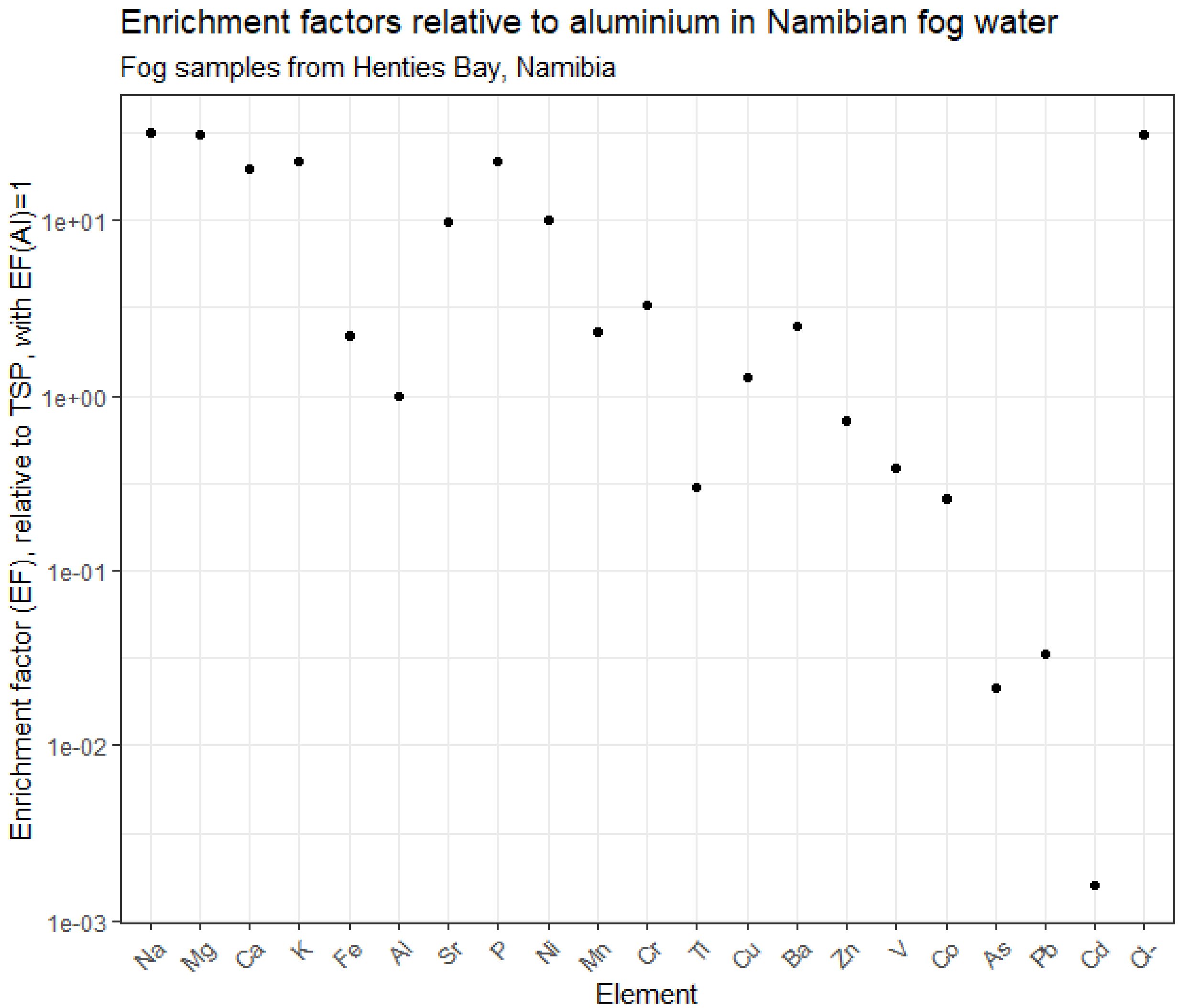

Figure S5. Crustal influence on fog chemical composition: enrichment factors for nss elements calculated relative to nss-Al measured in TSP on the Volume Weighted Concentrations for all fog samples collected at Henties Bay.

Figure S5 shows that Ti, V, Co, Cu, Zn, As, Cd, Nd, and Pb are mostly from crustal sources. Interestingly, Fe, P, Ca, Cr, Mn, Fe, Ni, and Sr do not appear to be exclusively from crustal sources and extra sources are to be looked for these elements. These results explain the observed higher fog concentrations of these elements as compared to seawater content (Table 2 and Table S1).

However, they should be moderated by two facts: i) the EFs were calculated using Al as the tracer, but the EF values obtained are in some cases below 1 indicating that extra sources may impact Al concentrations, and ii) the region is known to bear various mining activities that can contribute locally to influence some of the elemental ratios (Formenti et al, this issue). Although V and Ni (generally considered tracers for ship emissions) are observed in the coastal fogs at much higher concentrations than in seawater (Table 2), very low V / Ni ratios (0.03 with r^2=0.90) denote a very different source than ship emissions (for which typical ratios vary from 2.3 to 4.5; (Viana et al., 2009, 2014)). Finally, sulphate appears to be predominantly from marine sources (primary and secondary). Therefore, no detectable influence of ship emissions is observed, in good agreement with other studies during the campaign (see (Formenti et al., 2019; Giorio et al., 2022; Klopper et al., 2020)).

S4. Correlations

Table S2. Correlations (r) between aerosol pH, aerosol liquid water (ALW) content, temperature and relative humidity.

	pH	*ALW*	*T*	*RH*
pH	1.00			
ALW	0.72	1.00		
T	-0.21	-0.06	1.00	
RH	0.68	0.31	-0.11	1.00

Table S3. Correlations (r) between soluble elements in TSP and aerosol pH, aerosol liquid water (ALW) content, temperature and relative humidity.

	Al	*B*	*Ca*	*K*	*Mg*	*Na*	*Ba*	*Be*	*Co*	*Cu*	*Fe*	*Mn*	*Ni*	*P*	*Si*	*Sr*	*Ti*	*V*	*Zn*
pH	0.00	0.10	-0.48	-0.30	-0.31	-0.17	-0.51	0.03	-0.15	-0.27	-0.02	-0.45	-0.34	-0.40	-0.01	-0.35	0.01	-0.44	0.34
ALW	-0.14	-0.02	-0.18	-0.10	-0.11	-0.02	-0.22	-0.05	0.01	0.04	-0.13	-0.15	-0.18	-0.29	-0.11	-0.12	-0.08	-0.15	0.05
T	**-0.56**	0.49	0.43	0.59	0.57	0.65	0.14	0.16	0.04	0.28	**-0.47**	-0.06	0.02	0.28	-0.36	0.55	-0.38	0.32	0.11
RH	-0.04	0.23	-0.21	-0.02	-0.03	0.03	-0.48	0.17	-0.29	-0.24	-0.04	-0.51	-0.22	-0.11	-0.09	-0.07	0.02	-0.49	0.28

Table S4. Correlations (r) between major ions, organic and elemental carbon in TSP, and aerosol pH, aerosol liquid water (ALW) content, temperature and relative humidity.

	Na^+	K^+	Ca^{2+}	Mg^{2+}	Cl^-	SO_4^{2-}	nss- SO_4^{2-}	NH_4^+	*MSA*	NO_3^-	Br^-	*oxalate*	*formate*	*OC*	*EC*
pH	-0.15	-0.33	-0.48	-0.32	-0.15	-0.34	-0.38	-0.27	0.20	-0.43	-0.24	-0.36	-0.17	-0.37	-0.04
ALW	0.00	-0.11	-0.18	-0.11	0.00	-0.12	-0.15	-0.03	0.15	-0.07	-0.04	-0.26	0.01	-0.14	-0.16
T	0.67	0.58	0.45	0.57	0.70	0.61	0.57	0.51	-0.16	0.57	0.39	-0.24	0.56	0.26	0.29
RH	0.01	-0.07	-0.22	-0.05	0.07	-0.05	-0.07	-0.21	0.23	-0.33	0.07	-0.51	0.08	-0.21	0.09

Table S5. Correlations (r) between soluble elements (in %) and aerosol pH, aerosol liquid water (ALW) content, temperature, and relative humidity

	Al	*Ca*	*Mg*	*Co*	*Cr*	*Cu*	*Fe*	*Mn*	*Ni*	*P*	*Si*	*Sr*	*Ti*	*V*	*Zn*
pH	-0.02	0.23	-0.17	0.04	0.08	-0.19	0.12	0.26	-0.27	-0.21	-0.03	0	-0.01	0	0.35
ALW	-0.15	0.15	-0.08	-0.04	-0.06	-0.01	-0.08	0.52	-0.19	-0.34	-0.13	-0.01	-0.09	-0.07	0.02
T	-0.6	-0.09	0.09	-0.13	-0.44	-0.11	-0.5	-0.25	-0.3	-0.07	-0.45	-0.17	-0.38	-0.09	-0.14
RH	-0.15	0.21	0.09	-0.09	0.15	-0.18	-0.01	-0.08	-0.28	0.15	-0.2	0.14	-0.02	-0.23	0.31

S5. Additional speciation results

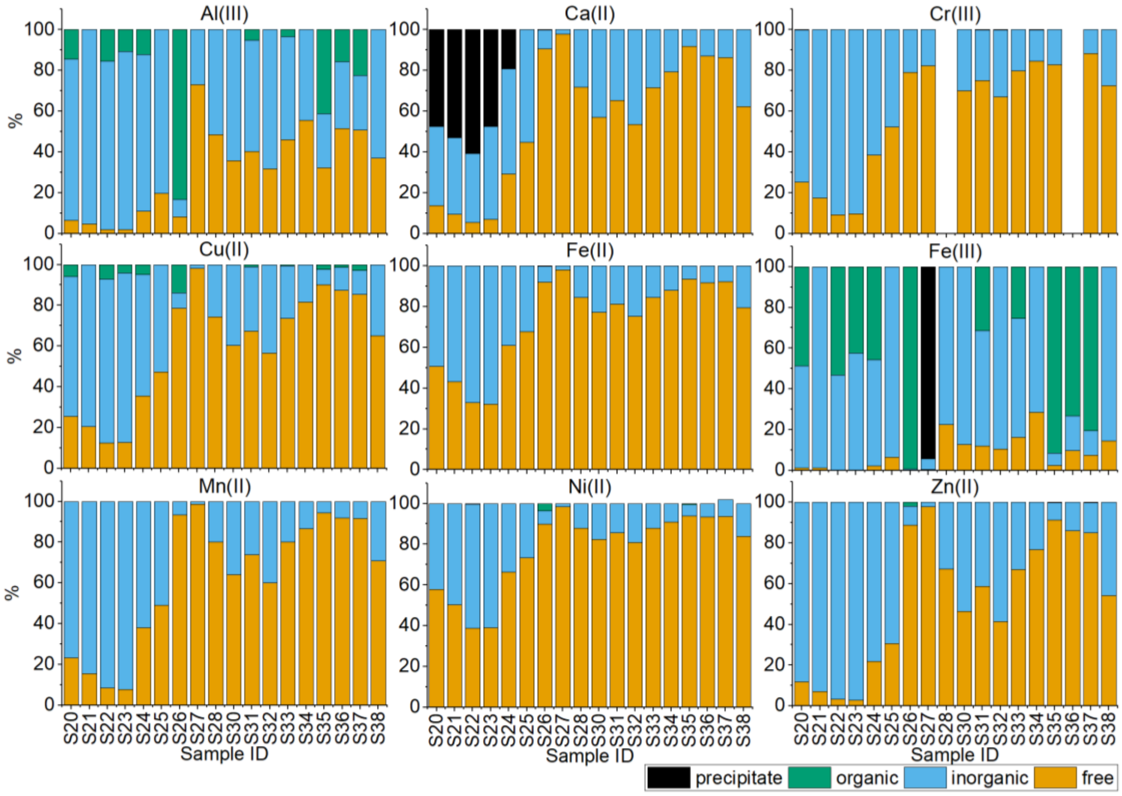

Figure S6. Speciation of soluble metals in ALW in TSP from Henties Bay (Namibia) obtained using the model Visual MinteQ for (a) Al(III), (b) Ca(II), (c) Cu(II), (d) Fe(II), (e) Fe(III), (f) Mg(II), (g) Mn(II), (h) Ni(II), and (i) Zn(II). Samples shown cover the period 3-12 September 2017.

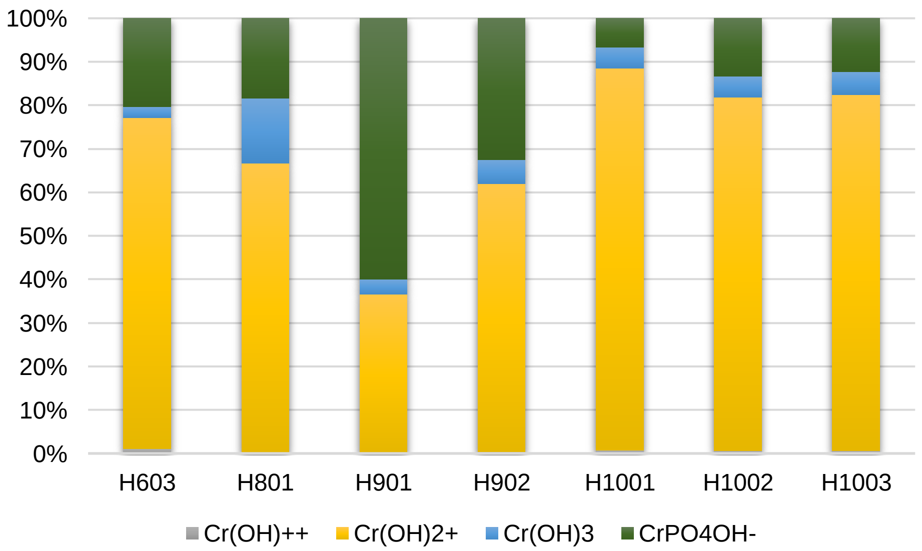

Figure S7. Detailed speciation of soluble Cr(III) in fog samples.

References

Formenti, P., D’Anna, B., Flamant, C., Mallet, M., Piketh, S. J., Schepanski, K., Waquet, F., Auriol, F., Brogniez, G., Burnet, F., Chaboureau, J.-P., Chauvigné, A., Chazette, P., Denjean, C., Desboeufs, K., Doussin, J.-F., Elguindi, N., Feuerstein, S., Gaetani, M., Giorio, C., Klopper, D., Mallet, M. D., Nabat, P., Monod, A., Solmon, F., Namwoonde, A., Chikwililwa, C., Mushi, R., Welton, E. J., and Holben, B.: The Aerosols, Radiation and Clouds in Southern Africa Field Campaign in Namibia: Overview, Illustrative Observations, and Way Forward, Bull Am Meteorol Soc, 100, 1277–1298, https://doi.org/10.1175/BAMS-D-17-0278.1, 2019.

Giorio, C., Doussin, J. F., D’Anna, B., Mas, S., Filippi, D., Denjean, C., Mallet, M. D., Bourrianne, T., Burnet, F., Cazaunau, M., Chikwililwa, C., Desboeufs, K., Feron, A., Michoud, V., Namwoonde, A., Andreae, M. O., Piketh, S. J., and Formenti, P.: Butene Emissions From Coastal Ecosystems May Contribute to New Particle Formation, Geophys Res Lett, 49, https://doi.org/10.1029/2022GL098770, 2022.

Klopper, D., Formenti, P., Namwoonde, A., Cazaunau, M., Chevaillier, S., Feron, A., Gaimoz, C., Hease, P., Lahmidi, F., Mirande-Bret, C., Triquet, S., Zeng, Z., and Piketh, S. J.: Chemical composition and source apportionment of atmospheric aerosols on the Namibian coast, Atmos Chem Phys, 20, 15811–15833, https://doi.org/10.5194/acp-20-15811-2020, 2020.

Viana, M., Amato, F., Alastuey, A., Querol, X., Moreno, T., Dos Santos, S. G., Herce, M. D., and Fernández-Patier, R.: Chemical tracers of particulate emissions from commercial shipping, Environ Sci Technol, 43, 7472–7477, https://doi.org/10.1021/es901558t, 2009.

Viana, M., Hammingh, P., Colette, A., Querol, X., Degraeuwe, B., Vlieger, I. de, and van Aardenne, J.: Impact of maritime transport emissions on coastal air quality in Europe, https://doi.org/10.1016/j.atmosenv.2014.03.046, 2014.